Jpn. J. Appl. Phys. Vol. 38 (1999) pp. 4936–4941
Part 1, No. 8, August 1999
©1999 Publication Board, Japanese Journal of Applied Physics

Measurement of Parameters for Simulation of 193 nm Lithography Using Fourier Transform Infrared Baking System

Atsushi SEKIGUCHI, Mariko ISONO and Toshiharu MATSUZAWA
Litho Tech Japan Corp., 2-6-6, Namiki, Kawaguchi, Saitama, 332-0034, Japan

(Received November 28, 1998; accepted for publication May 10, 1999)

By incorporating baking equipment into a Fourier transform infrared (FT-IR) spectrometer, a deprotection reaction parameter measurement system that can be used with chemically amplified resists has been developed. This system allows us to study new models for chemically amplified (CA) resists by including into a conventional deprotection reaction model an initial delay effect and a quencher effect. This model is also used to measure deprotection reaction parameters. The parameters thus obtained are inputted into a lithography simulator PROLITH/2 to perform profile simulations. The results are compared with those of scanning electron microscope (SEM) observations. Although the simulation results and SEM observations are not in complete agreement, the general trends observed are in adequate agreement. These results confirm the applicability of the proposed model to CA resists for ArF excimer laser lithography and verify the usefulness of the measurement system.

KEYWORDS: FT-IR spectrometer, chemically amplified resist, post-exposure bake, simulation parameters, deprotection reaction rate constant, deprotection reaction order, quencher concentration, lithography simulation

1. Introduction

In ArF excimer laser lithography, polyhydroxystyrene (PHS), which is used in the conventional KrF excimer laser process, cannot be used due to the extremely intense absorption at the exposure wavelength (193 nm).[1] Therefore, ArF excimer laser processes require the development of new resist materials. In general, lithography simulation is a useful tool to aid the development of new materials.[2] During the post-exposure bake (PEB) of a chemically amplified (CA) resist, the acid generated by the exposure diffuses, and the deprotection reaction occurs. Since the concentration of the protection groups determines the solubility of the resist in the developer, the simulation parameters related to the deprotection reaction have significant influence on the accuracy of profile simulations of CA resists.

By incorporating baking equipment into a Fourier transform infrared (FT-IR) spectrometer, we developed a system that performs *in situ* infrared spectral analysis of changes in the deprotection reaction during PEB. Using this system, we have successfully determined the simulation parameters associated with the deprotection reaction: the deprotection reaction rate constant K_{dp}, the deprotection reaction order m, the photoacid generator (PAG) reaction constant C (Dill's C), the parameter related to quencher concentration B, and the deprotection initial delay constant T_d. The deprotection reaction model[3] developed by Ohfuji *et al.* and his colleagues was used as the basis of the modeling. The parameters obtained were inputted into a lithography simulator PROLITH/2[4] to calculate the profiles of 0.15 μm line-and-space features. The simulation results were compared with the SEM observations of actual, printed patterns to verify the effectiveness of the analysis system and the modeling.

2. Hardware Configuration

Figure 1 shows the appearance of the hardware system that was used in this study. The FT-IR spectrometer used was the FTS-135 made by Bio-Rad Corporation. A bake plate, with a 10-mm-diameter hole located at the center to let IR light through, was attached perpendicular to the light path in the measurement chamber of the FT-IR spectrometer. Measurements were performed in the transmission mode. The area of the measurement was approximately 5 mm in diameter.

The wafer was fixed to the transfer shuttle unit by vacuum suction, and the wafer was moved to the bake plate within 0.5 s after the start button was pressed. Proximity baking with a gap of about 0.2 mm was employed. When the baking was started, *in situ* IR measurement was started simultaneously. The baking temperature was controlled within ±0.3°C on the wafer surface. The existence of a 10-mm-diameter hole did not cause any detectable nonuniformity in the temperature distribution.

IR measurements were conducted with a wave number resolution of 4 cm^{-1} over a range of 500 to 2000 cm^{-1}. Measurement scan was carried out once, and sampling was done every 2 s.

3. Calculation Model

Figure 2 shows the structural formulae for the resist materials that were used in the study. The resist resin was a terpolymer composed of tertiary butyl methacrylate (TBMA), isobornyl methacrylate (IBMA), and methyl methacrylate (MMA). The photoacid generator was triphenylsulphonium triflate (TPS). A t-butyl group was used as the protection group. Figure 3 shows the assumed deprotection reaction of the protection group. Figure 4 shows an infrared absorption spectrum vs PEB time at wave numbers 500–2000 cm^{-1}. The absorption peak at 1144 cm^{-1} for the C–O bond (ester bond) between the protection group and the resin decreases in size as a function of PEB time.

In the next step, the absorbance at the wave number that was measured under various conditions was normalized by the absorbance of the completely reacted material with a sufficient exposure dose to give the protection ratio $[P]$. By analyzing data obtained in this fashion (decreases in intensity of the ester absorption band in the IR spectrum) using a simulator which adopts a stochastic mechanism, Wallraff *et al.*[5] showed that the kinetic parameters can be obtained. They used TMBA polymer with triphenylsulfonium hexafluoroantimonate ($TPS\text{-}SbF_6$) as PAG in deprotection reaction analyses employing an FT-IR spectrometer (focusing on the decrease in intensity of the t-butyl infrared absorption band at 1369 cm^{-1}). The deprotection reaction (acid-catalyzed deprotection) was treated using a model based on first-order re-

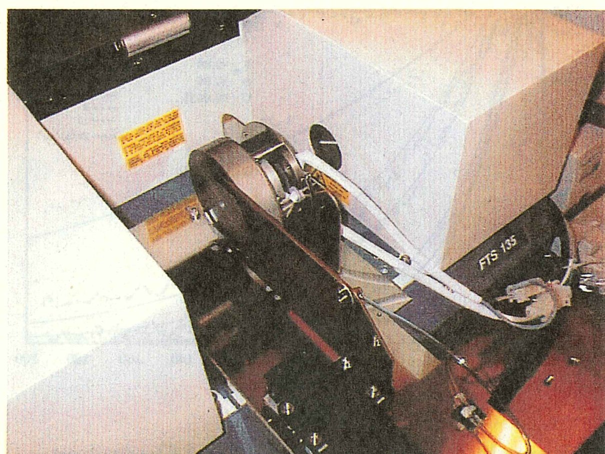

Fig. 1. External view of the FT-IR and bake system.

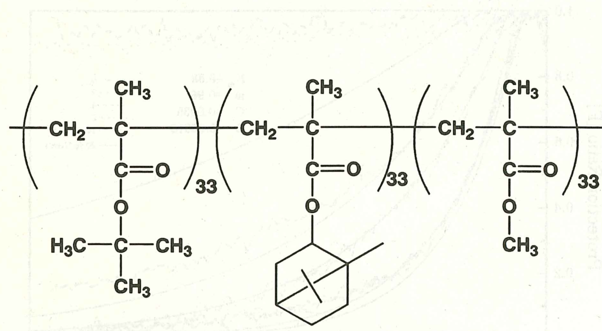

(a)($TBMA_{0.33}$-$IBMA_{0.33}$-$MMA_{0.33}$) Polymer

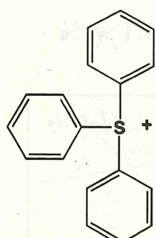

(b)(TPS) Photoacid generator

Fig. 2. Chemical structure of a chemically amplified positive resist.

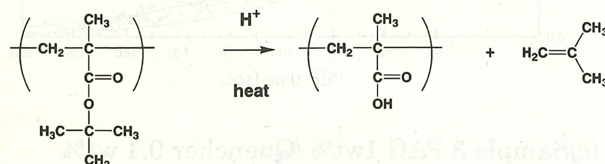

Fig. 3. The expected deprotection reactions.

action kinetics, and reaction constants were extracted using a new model which adds a proton transfer step between the unreacted groups and the reaction products.[5] The technique for deprotection reaction analysis described by Wallraff *et al.* is a useful method for gaining a qualitative understanding of the kinetics of the deprotection reaction.

On the other hand, Ohfuji *et al.*[3] described a model which gives a quantitative treatment of the deprotection reaction. The model of Ohfuji *et al.* is as follows.

$$[P] = \exp[K_{\rm dp}\{1 - \exp(-CE)\}^m t] \qquad (1)$$

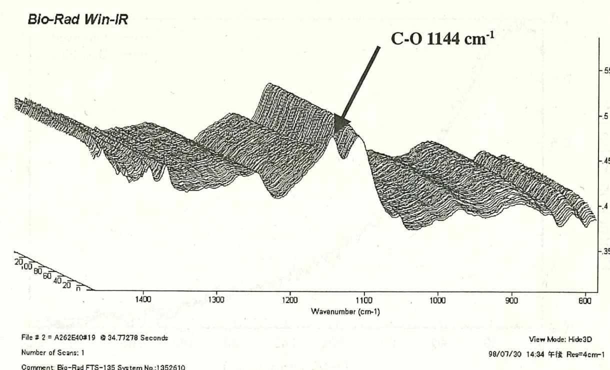

Fig. 4. Typical FT-IR difference spectra showing deprotection reaction as a function pf PEB time.

where:
$[P]$: Normalized concentration of protection group,
$[\mathrm{H}^+]$: Normalized concentration of acid,
$K_{\rm dp}$: Deprotection reaction constant/s^{-1},
m: Deprotection reaction order,
C: PAG reaction constant/cm^2 mJ^{-1},
E: Exposure dose/mJcm^{-2},

The purpose of this study was to extract parameters for use in the quantitative analysis of the deprotection reaction using a lithography simulator. To this end, we adopted the deprotection reaction model of Ohfuji *et al.*

We added an initial delay term for the deprotection reaction and an acid loss term due to the quencher into the Ohfuji Model [eq. (1)].

The new model is given by [eq. (2)].

$$[P] = \exp\{-K_{\rm dp}[\mathrm{H}^+]^m(t - T_{\rm d})\} \qquad (2)$$

where:

$$[\mathrm{H}^+] = 1 - \exp(-CE) - CEQ$$

$T_{\rm d}$: Initial delay constant for the deprotection reaction/s,
Q: Decrease in acid concentration due to the presence of base quencher,

After the wafer is set on the bake plate and PEB begins, it takes 5 to 8 s for the wafer to reach the specified temperature. The initial delay effect in the deprotection reaction refers to the phenomenon in which the delay in temperature rise on the wafer results in a delay in the start of the reaction. This effect has been observed for the first time in this study as a result of *in situ* measurements.

Further more, when a quencher exists in the resist, the quencher captures the acid generated upon exposure. If there is no acid generation resulting from exposure, then the quencher cannot capture the acid. Hence it appears that the amount of acid captured by the quencher is proportional to the exposure energy and the PAG reaction constant. Figure 5 shows an example of the curve fitted using eq. (2).

4. Experiment and Results

The following three samples were used to calculate the simulation parameters and to verify the accuracy of the proposed modeling equation. They were the mixtures of terpolymer resin composed of TBMA, IBMA and MMA (TBMA : IBMA : MMA = 1 : 1 : 1), and a photoacid generator TPS. An aniline derivative was used as quencher and PGMEA was

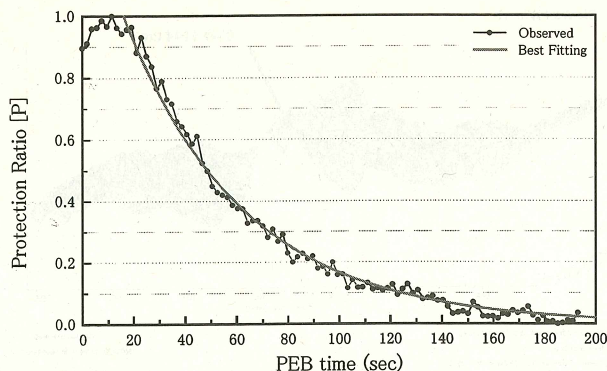

Fig. 5. A normalized protection ratio calculated from FT-IR spectra as a function of PEB time.

used as solvent. The sample compositions were as follow:

Sample 1: PAG, 2 wt% relative to resin, without quencher

Sample 2: PAG, 2 wt% relative to resin, with quencher 0.1 wt% relative to resin

Sample 3: PAG, 1 wt% relative to resin, with quencher 0.1 wt% relative to resin

The film thickness was 0.5 μm for all samples. The prebake was carried out at 120°C for 60 s. The ArF exposure system ArFES-3000[6] was used for the exposure. Figure 6(a) and 6(b) (dotted lines) show the relationship between the protection ratio and the PEB time at exposure doses of 0, 2, 4, 6, 10 and 20 mJ/cm^2 for Samples 1 and 2. In Sample 1, with no quencher added, the deprotection reaction proceeded at the dose of 2 mJ/cm^2. In contrast, there was little deprotection reaction at the dose of 2 mJ/cm^2 in Sample 2 that contained 0.1 wt% of quencher. At exposure doses higher than 10 mJ/cm^2, there was no significant difference in the deprotection reaction between the two samples.

This suggests that in the low exposure dose region, the addition of a quencher results in the inhibition of the deprotection reaction due to the capture of acid, whereas in the high exposure dose region, the quencher does not significantly affect the deprotection reaction. In other words, the addition of the quencher improves the effective resist contrast. The solid lines show the results of the fitting using the proposed equation (2). The curves for Sample 1 are in good agreement with the observed data.

For Sample 2, the effects of the quencher are obvious at the exposure dose of 2 mJ/cm^2. Although there is some deviation from the observed data at 2 mJ/cm^2, the results are in good agreement at doses greater than 4 mJ/cm^2 when the quencher constant of $B = 0.03016$ is used. Figure 6(c) shows the relationship between the protection ratio and PEB time for Sample 3 at exposure doses 0, 2, 4, 6, 10 and 20 mJ/cm^2. As the PAG concentration decreased from 2 wt% to 1 wt%, a deprotection reaction began at 4 mJ/cm^2 at the PAG concentration of 2 wt%. In contrast, at the PAG concentration of 1 wt%, an exposure dose of 6 mJ/cm^2 is required for the deprotection reaction to begin. These results indicate that the amount of the deprotection reaction decreases as a function of PAG concentration. The solid lines represent the fitted curves. With a quencher constant of $B = 0.04300$, there is a general agreement between simulated and observed data.

The deprotection reaction model shown in this study gives an adequate degree of agreement at different PAG concentrations with and without the quencher. Therefore, the model is considered valid for the materials used in the study.

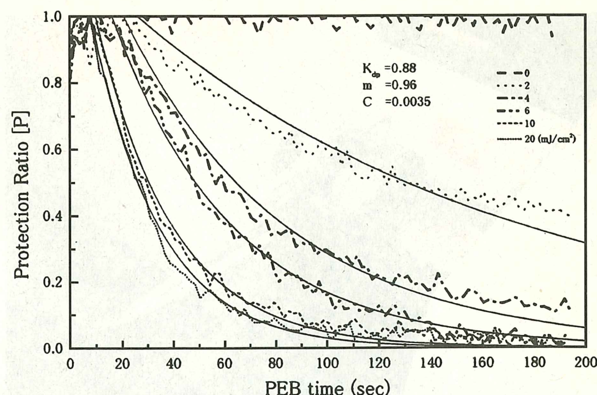

(a)Sample 1 PAG 2 wt% /Without Quencher

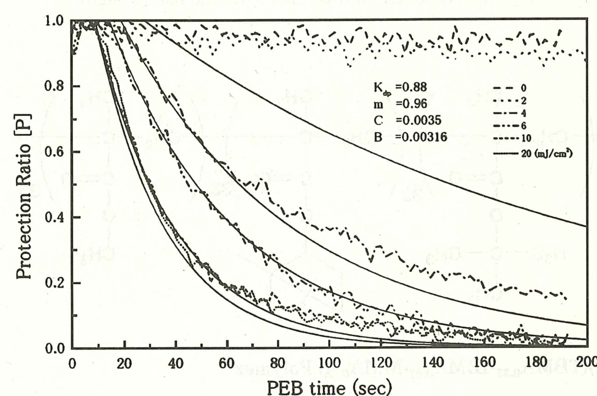

(b)Sample 2 PAG 2 wt% /Quencher 0.1 wt%

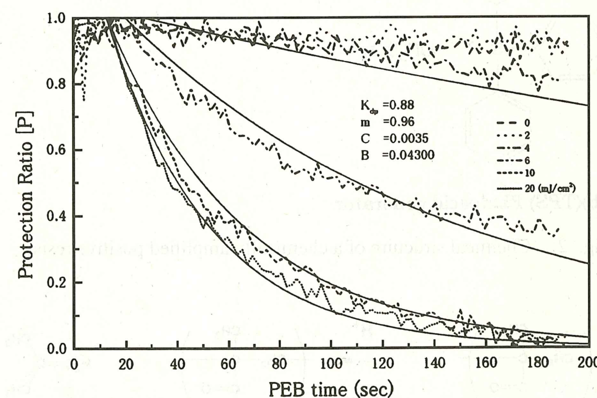

(c)Sample 3 PAG 1wt% /Quencher 0.1 wt%

Fig. 6. Relationship between $[P]$ and PEB time for different exposure dose.

Figure 7 shows the relationship between the exposure dose and the initial delay constant for the deprotection reaction ("delay constants") for various samples. The higher the exposure dose is, the smaller the delay constant. This suggests that an increase in the exposure dose produces a greater number of H$^+$, causing the deprotection reaction to begin even at low temperatures.

Figures 8(a), 8(b), and 8(c) show the deprotection reaction

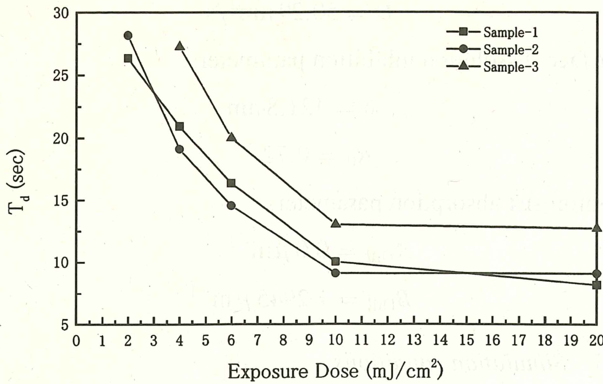

Fig. 7. Relationship between T_d and exposure dose for different sample.

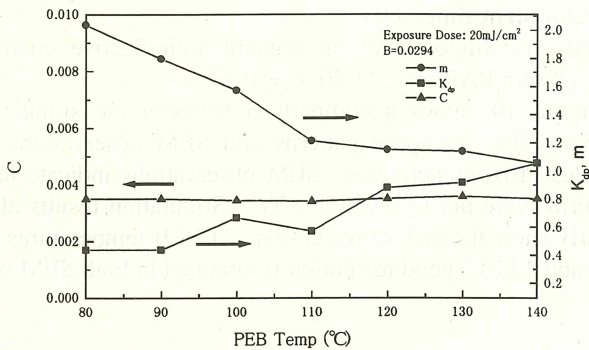

(a)Sample 1 PAG 2 wt% /Without Quencher

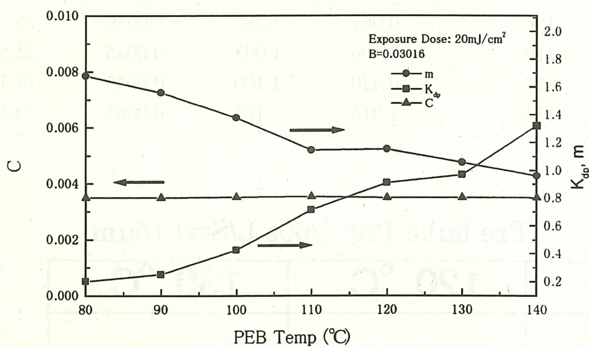

(b)Sample 2 PAG 2 wt% /Quencher 0.1 wt%

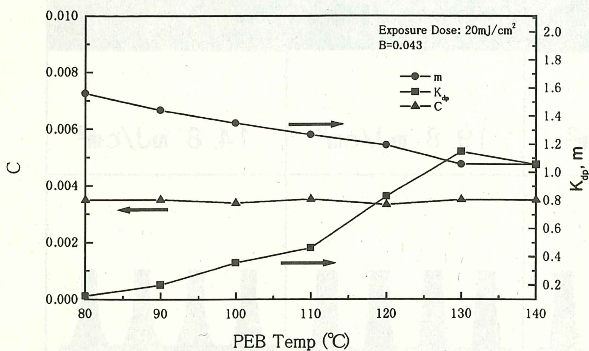

(c)Sample 3 PAG 1wt% /Quencher 0.1 wt%

Fig. 8. Relationship of K_{dp}, m and C with PEB temperatures.

constant K_{dp}, the deprotection reaction order m, and the PAG reaction constant C for Samples 1, 2, and 3 at various PEB temperatures. All samples indicate that the deprotection reaction constant K_{dp} tends to increase ($0.2 \rightarrow 1.2$) as a function of PEB temperature. From this, we concluded that as the PEB temperature rises, the deprotection reaction proceeds more efficiently. On the other hand, the deprotection reaction order m tends to decrease ($1.8 \rightarrow 1.0$). This indicates that the higher the PEB temperature, the more activated is the reaction in which the acid acts as a catalyst, suggesting that a reaction similar to an acid-amplified reaction takes place. From this it is surmised that as the PEB temperature rises, the deprotection reaction will proceed still more efficiently. The PAG reaction constant C depends only on the exposure, and is independent of the PEB temperature; for this reason, a value of about 0.0035 was obtained for all samples. The PAG reaction constant C is approximately constant (about 0.0035).

5. Simulation

To examine the usefulness of the model from the standpoint of the profile simulation, we used a commercially available CA resist, PAR-101A4, for which PAG and quencher concentrations were optimized. The simulation parameters obtained were inputted into the PROLITH/2 to perform 0.15 μm line-and-space patterns simulations. Then, the results were compared with SEM observations of resist images that were printed using a stepper.

The parameters were measured under the following conditions.

5.1 *Parameter measurement conditions*

Resist: PAR-101A4 (Sumitomo Chemical)
Film thickness: 0.50 μm
Prebake: 120°C–60 s
PEB: 100, 110, 120 and 130°C
Developer: NMD-3 (TMAH 2.38%) 23°C

Figure 9(a) shows the relationship between the protection ratio and PEB time at different PEB temperatures. At 100°C, the deprotection reaction was not completed even after 200 s. However, at PEB temperatures higher than 110°C, the deprotection reaction is completed in 200 s. The solid lines, which indicate the results of fitting, are in good agreement with the observed data.

Figure 9(b) shows the relationship between PEB temperature, and the deprotection reaction constant K_{dp}, the deprotection reaction order m, and the PAG reaction constant C (observed values are listed in Table I). The quencher constant B was 0.00205 for all of other parameters.

The Resist Development Analyzer RDA-790[7] was used to measure the development rate. The ABC-Analyzer[8] was used to measure the photoresist absorption parameter B_{Dill}. The PAG diffusion coefficient D, and the surface dissolution inhibition parameters δ (inhibition depth) and R_0 (real surface rate) were calculated using DPC-Software.[9] The measured parameters other than those related to the deprotection reaction were as follows.

5.2 *Results of parameter measurements*

Development parameters for the Original Mack model:

$$R_{max} = 198\,\text{nm/s}$$

$$R_{\min} = 0.003\,\text{nm/s}$$

$$n = 14.6$$

$$m_{\text{TH}} = 0.985$$

PAG diffusion coefficient:

$$D = 50.29\,\text{nm}^2/\text{s}$$

Surface dissolution inhibition parameters:

$$\delta = 121.8\,\text{nm}$$

$$R_0 = 0.72$$

Photoresist absorption parameter:

$$A_{\text{Dill}} = 0.0\,\mu\text{m}^{-1}$$

$$B_{\text{Dill}} = 1.2945\,\mu\text{m}^{-1}$$

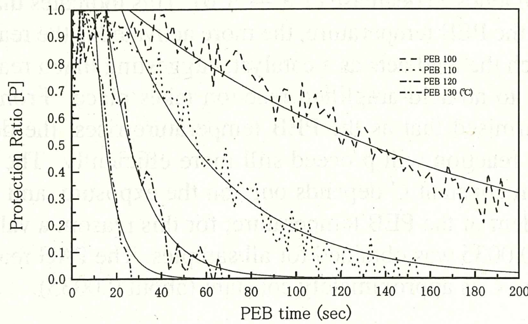

(a)Relationship between [P] and PEB time for different PEB time.

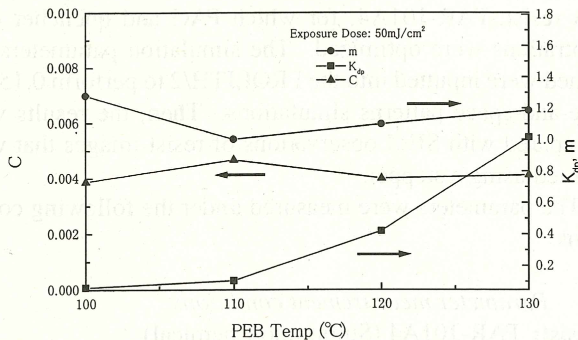

(b) Relationship between K_{dp}, m and C for different PEB time.

Fig. 9. Analysis result regarding deprotection reactions of PAR-101A4.

5.3 *Simulation conditions*

Exposure wavelength: 193 nm
NA: 0.60 (assuming a stepper made by ISI Corp.)
Coherence factor: 0.70
Line and space: 0.15 μm
Development time: 60 s
Substrate: Silicon with an organic antireflective coating (80 nm BARC/$n = 1.80$, $k = 0.37$)

Figure 10 shows a comparison between the simulated 0.15 μm line-and-space patterns and SEM observations at various PEB temperatures. SEM observations indicate that patterns were not resolved at 100°. Simulation results also clearly show the lack of resolution. At PEB temperatures of 110 and 120°C, good resolution is obtained in both SEM ob-

Table I. PEB parameters for PAR-101A4 resist with PEB temperature varied.

PEB Temp. (°C)	K_{dp}	m	C	T_d
100	0.061	1.280	0.0039	25.29
110	0.106	1.003	0.0046	22.59
120	0.420	1.100	0.0043	15.33
130	1.016	1.185	0.0063	10.35

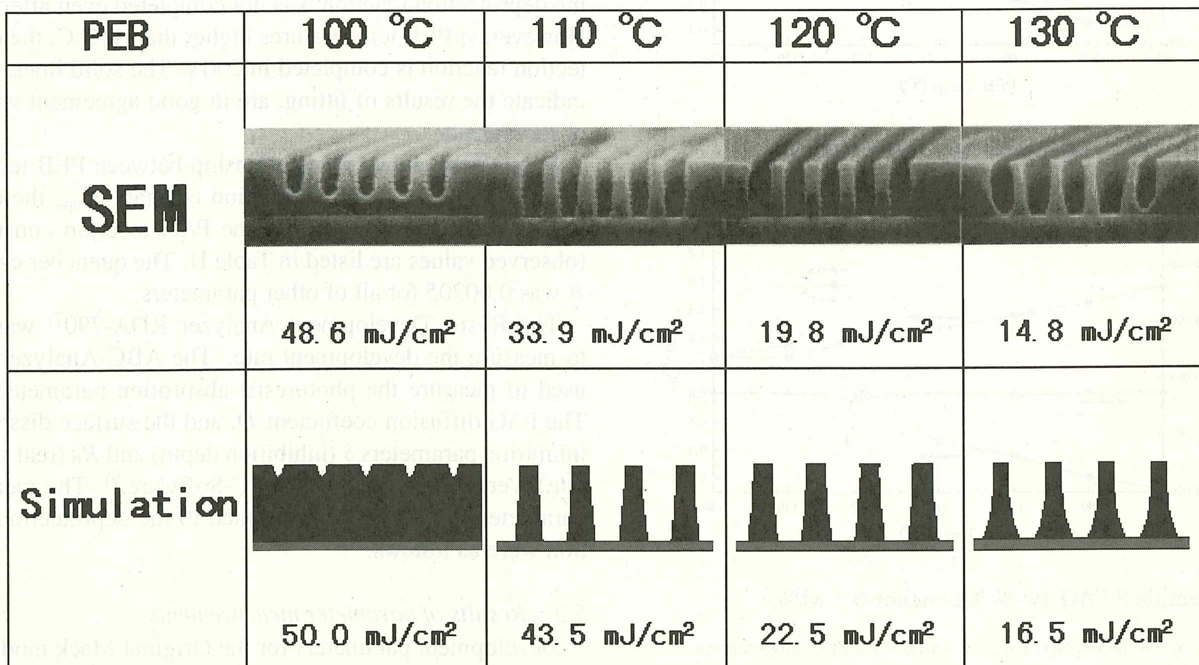

Fig. 10. Comparison between simulated profiles and SEM observations.

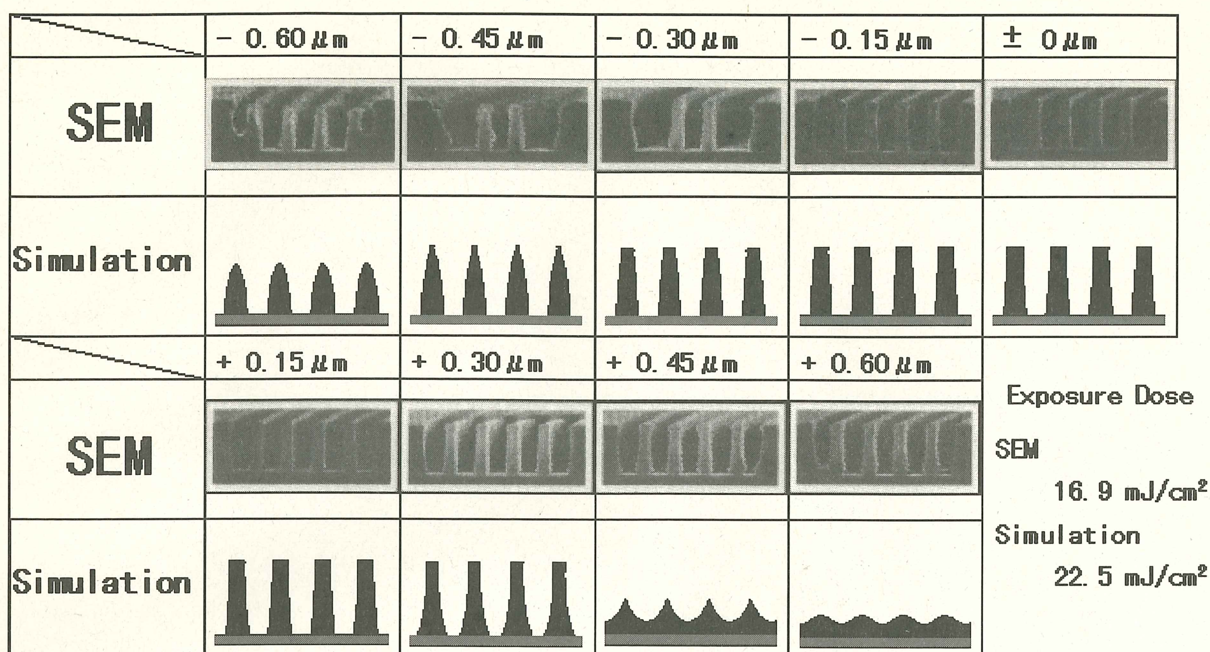

Fig. 11. Comparison between simulated profiles and SEM observations.

servations and simulations.

At 130°C, footers appeared in the actual resist profile. Although the agreement was not perfect, the simulated profile also showed footers.

The actual resist patterns also showed an increase in sensitivity as a function of PEB temperature. The same trend was reproduced in the simulations. This suggests that the sensitivity is increased by the increase in the deprotection reaction constant K_{dp} which is a function of PEB temperature. Figure 11 shows a comparison between SEM observations and simulations for the focus range of -0.60 to $+0.60\,\mu$m at 120°C. While the agreement was not very good on the + defocusing side, the results are in fair agreement on the − defocusing side, resulting in a good overall agreement. These results demonstrate that the deprotection model presented in this report is applicable to the ArF resist.

6. Conclusion

A baking apparatus was incorporated into an FT-IR system in order to develop a measurement system for the deprotection reaction parameters. The system was used to verify the deprotection reaction model by using a CA resist for ArF lithography. A commercial resist with optimized PAG and quencher concentrations was used to measure the profile simulation parameters. Profile simulations were performed by using the PROLITH/2, and the results were compared with SEM observations. Although simulation results and SEM observations were not in complete agreement, the overall trend obtained was in adequate agreement. These results confirmed the applicability of the measurement system to CA resists for ArF lithography.

Acknowledgements

The authors would like to express their sincere appreciation to Yasunori Uetani of Precision Chemical Laboratories, Sumitomo Chemical Co., Ltd. for providing the resist materials. The authors would also like to express their gratitude to Dr. Takeshi Ohfuji of Semiconductor Leading Edge Technologies, Inc. and Dr. Vivek Singh of Intel Corporation, who gave valuable advice on the deprotection reaction model.

1) T. Naito, K. Asakawa, N. Shida, T. Ushirogouchi and M. Nakase: Jpn. J. Appl. Phys. **33** (1994) 7028.
2) R. A. Fergason, J. M. hutchinson, C. A. Spence and A. R. Neureuther: J. Vac. Sci. Technol. B **8** (1990) 1423.
3) T. Ohfuji, A. G. Timko, O. Nalamasu and D. R. Stone: Proc. SPIE **1925** (1993) 213.
4) C. A. Mack: Proc. SPIE **538** (1985) 207.
5) G. Wallraff, J.Hinsberg, F. Houle, P. Seidel, R. Johnson and W. Oldham: J. Vac. Sci. Technol. B **12** (1994) 3857.
6) A. Sekiguchi, M. Kadoi, T. Matsuzawa and Y. Minami: Semicond. World **6** (1997) 25.
7) A. Sekiguchi, C. A. Mack, Y. Minami and T. Matuzawa: Proc. SPIE **2725** (1995) 49.
8) A. Sekiguchi, Y. Minami, T. Matsuzawa, T. Takezawa and H. Miyakawa: Electron. & Commun. Jpn. Pt. 2 **78** (1997) 21.
9) A. Sekiguchi, M. Kadoi, T. Matsuzawa and Y. Minami: Electron. & Commun. Jpn. Pt. 2 **J81** (1998) 542.